

# The Adsorption Geometry and Electronic Structure of Organic Dye Molecule on TiO<sub>2</sub>(101) Surface from First Principles Calculations

Mang Niu<sup>1,a</sup>

<sup>1</sup>College of Science, China University of Petroleum (East China), Qingdao 266580, Shandong Province, China

**Abstract.** Using density functional theory (DFT), we have investigated the structural and electronic properties of dye-sensitized solar cells (DSSCs) comprised of I-doped anatase TiO<sub>2</sub>(101) surface sensitized with NKX-2554 dye. The calculation results indicate that the cyanoacrylic acid anchoring group in NKX-2554 has a strong binding to the TiO<sub>2</sub>(101) surface. The dissociative and bidentate bridging type was found to be the most favorable adsorption configuration. On the other hand, the incorporations of I dopant can reduce the band gap of TiO<sub>2</sub> photoanode and improve the of NKX-2554 dye, which can improve the visible-light absorption of anatase TiO<sub>2</sub> and can also facilitate the electron injection from the dye molecule to the TiO<sub>2</sub> substrate. As a result, the I doping can significantly enhance the incident photon-to-current conversion efficiency (IPCE) of DSSCs.

## 1 Introduction

Dye-sensitized solar cells (DSSCs) have been attracting much attention because of their high energy conversion efficiency and as a low-cost alternative to commercial solar cells based on silicon.[1,2] In the past decades, great efforts have been made to further improve the energy conversion efficiency in order to commercialize DSSCs successfully. One of the key elements in DSSCs is the semiconductor photoanode, which composed of anatase TiO<sub>2</sub> nanocrystals. The TiO<sub>2</sub> photoanode transfers photoexcited electrons from the dye molecules to the transparent conducting substrate and concurrently allows the electrolytes to diffuse to the anchored dyes.[3] However, such pure TiO<sub>2</sub> nanocrystalline films usually show poor light harvesting due to its wide band gap (3.2 eV for anatase TiO<sub>2</sub>). It is well known that enhancing the photocapture efficiency and optical absorption of the photoelectrode films can significantly improve the photon-to-current conversion efficiency of TiO<sub>2</sub>-based DSSCs.[4]

Recently, it is reported that the incident photon-to-current conversion efficiency (IPCE) and the overall conversion efficiency of DSSCs can be enhanced by using a non-metal (such as N and I) doped TiO<sub>2</sub> nanocrystalline as photoanode.[4-6] For example, Hou et.al observed that the photovoltaic performance of the DSSCs based on I-doped TiO<sub>2</sub> photoanode is 42.9% higher than that of the cell based on undoped TiO<sub>2</sub> photoanode.[6] The improved performance is explained by the expanded visible-light harvesting, lowered recombination resistance together with prolonged electron lifetime of I-doped TiO<sub>2</sub> photoanode. However, the fundamental physical processes of the IPCE enhancement in

<sup>a</sup> Corresponding author : niumang@upc.edu.cn

the DSSCs based on the I-doped TiO<sub>2</sub> photoanode is not understood completely yet, because the adsorption property of the dye sensitizer on I-doped TiO<sub>2</sub> photoanode and the electronic property of such adsorbed complexes have not been investigated fully.

It is well known that density functional theory (DFT) calculations have been widely used to investigate the adsorption and electronic properties of dye molecule on TiO<sub>2</sub> substrate. Therefore, we performing DFT calculations to discuss the origin of IPCE enhancement in the DSSCs based on the I-doped TiO<sub>2</sub> photoanode. [7] Firstly, we calculated the electronic structures of pure and I-doped TiO<sub>2</sub>(101) surfaces. Then, the absorption behavior of dye molecule on the pure and I-doped TiO<sub>2</sub>(101) surfaces and the electronic properties of adsorbed dye/TiO<sub>2</sub> complexes were investigated. Finally, the IPCE enhancement in the DSSCs based on the I-doped TiO<sub>2</sub> photoanode is discussed.

## 2 Calculation Methods

Our calculations were carried out using the Vienna Ab-initio Simulation Package (VASP)[8] with the generalized gradient approximation (GGA). The first principles pseudopotential were generated by the projector-augment-wave (PAW)[9] method. The Perdew-Burke-Ernzerhof (PBE)[10] of was adopted to describe the exchange and correlation functionals. The cutoff energy for the plane-wave basis set was set to 500 eV. A 3×3×1 Monkhorst-pack grid was used in the DFT calculations. For the geometry optimizations, the convergence criterion of forces on each ion was set to 0.01 eV/Å. The resulting structures were then used for the electronic structures calculations. Considering that the standard DFT often fails to predict the correct band gaps of transition metal oxides like TiO<sub>2</sub> due to the self-interaction error inherent in such functional, we adopted DFT+U method for geometry optimization and subsequent electronic structure calculations. The onsite U = 6.0 eV and J = 0.5 eV parameters were applied to the Ti-3d electrons.[11]

The adsorption of dye molecular on TiO<sub>2</sub> surface was simulated by using vacuum slab models. The TiO<sub>2</sub> surfaces were modeled by a 2×4 anatase TiO<sub>2</sub>(101) supercell along [101] and [010] directions with double-layer of slab. We fixed the bottom layer of slab during the geometry optimizations. A 25 Å vacuum region was used to ensure the decoupling between neighboring systems. The I-doped TiO<sub>2</sub>(101) slab was constructed by inducing I atom to the Ti site of TiO<sub>2</sub>. Such vacuum slab models have been used often in the theoretical calculations of DSSCs.[12] The polyene-dye of 2-Cyano-5,5-bis(4-dimethylaminophenyl)penta- 2,4-dienoic acid (NKX-2554) was used as the photosensitizer in our simulation models because such organic dye has shown high IPCE performance in DSSCs. The adsorption energy of NKX-2554 dye on TiO<sub>2</sub>(101) slab, E<sub>ads</sub>, is calculated using the expression

$$E_{ads} = E_{slab} + E_{dye} - E_{dye/slab} \quad (1)$$

where E<sub>slab</sub> is the energy of the clean TiO<sub>2</sub>(101) slab, E<sub>dye</sub> represents the energy of the NKX-2554 dye, and E<sub>dye/slab</sub> represents the total energy of the adsorbed dye/TiO<sub>2</sub> system. A positive value of E<sub>slab</sub> > 0 indicates stable adsorption.

## 3 Results and Discussion

### 3.1 I-doped anatase TiO<sub>2</sub>(101) surface

To explore the origin of IPCE enhancement in the DSSCs based on the I-doped TiO<sub>2</sub> photoanode, we first investigated how the incorporation of I-dopant affects the electronic structures of the anatase TiO<sub>2</sub>. The DFT+U calculated density of states (DOSs) of pure and I-doped anatase TiO<sub>2</sub>(101) surface were displayed in Fig. 1a and Fig1b, respectively. The highest occupied state is chosen as the Fermi energy and is displayed with a black dashed line. For the pure anatase TiO<sub>2</sub>(101) surface, its valence band (VB) and conduction band (CB) were separated by a wide gap. The valence band consists

mainly of O-2p states, including some hybridization with the Ti-3d orbital. The conduction band is dominated by Ti-3d states. Fig. 1b shows that the VB and CB of I-doped anatase TiO<sub>2</sub>(101) surface are the same as those of undoped TiO<sub>2</sub>. However, I-doping introduces a fully occupied band gap state 0.5 eV above the valence band maximum (VBM). The partial DOS plots shows that this band gap state consists mostly of I 5s states (not shown here) and the 2p-states of its neighboring O atoms, and that the I-5p states contribute to the conduction band. This indicates that I dopant on Ti site exists as an I<sup>5+</sup> (s2) cation, as found experimentally.[13] The calculated band gap energy is 2.62 and 1.73 eV for the pure and I-doped anatase TiO<sub>2</sub>(101) surface, respectively. Therefore, the effective band gap reduction of anatase TiO<sub>2</sub> photoanode through I doping can lead to a significant red-shift of optical absorption edge, which provides a natural explanation for the increased IPCE of DSSCs.

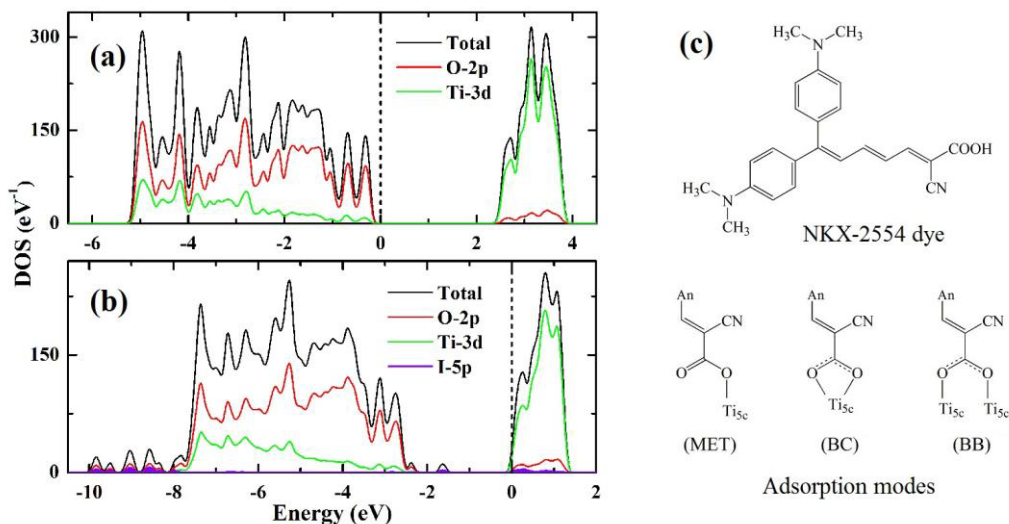


**Figure 1.** The DFT+U calculated DOSs for (a) pure and (b) I-doped anatase slabs. (c) The possible dissociative adsorption configurations of NKX-2554 dye on TiO<sub>2</sub>(101) surface.

In addition, the Fermi level of I doped TiO<sub>2</sub>(101) surface (Fig. 1b) is pinned at 0.16 eV above the conduction band minimum (CBM) so that iodine is effectively acting as an n-type dopant in TiO<sub>2</sub>, showing a typical n-type metallic characteristic. Therefore, it is suggested that the I-doping can improve the conductivity of anatase TiO<sub>2</sub> photoanode. In fact, the open-circuit voltage (V<sub>oc</sub>) of DSSCs is determined by the energy difference between the CBM of TiO<sub>2</sub> electrode and the reduction level of hole-transport material (HTM). The n-type I-doping lead to the increase of the electron concentration and upward shift of the CBM, as a result, the V<sub>oc</sub> of of DSSCs is enlarged. These results are consistent with the corresponding experimental findings.[6]

### 3.2 Adsorption of NKX-2554 dye on TiO<sub>2</sub>(101) surface

In addition to the high solar-cell performance of NKX-2554 dye, its prospective low-cost production owing to its simple molecular structure and synthesis procedure suggest a possibility of promising applications of organic-dye photosensitizers in DSSCs. The NKX-2554 dye is bestowed with a donor part (electron donating group), an acceptor part (electron accepting group) and an anchoring group. The cyanoacrylic acid anchoring group in NKX-2554 has a strong binding to the TiO<sub>2</sub> surface.[14] The adsorption of NKX-2554 dye on anatase (101) surface has been extensively studied to search for the energetically most favorable structure of adsorbed dye/TiO<sub>2</sub> systems.[15] The possible dissociative adsorption modes for the cyanoacrylic acid derivative are shown in Fig. 1c. The coordination may be monodentate ester-type (MET), bidentate chelating (BC), or bidentate bridging (BB) depending on the

number of oxygens used by the carboxylate anion (An-COO<sup>-</sup>) to coordinate the five-coordinated surface Ti (Ti5c) acidic sites.

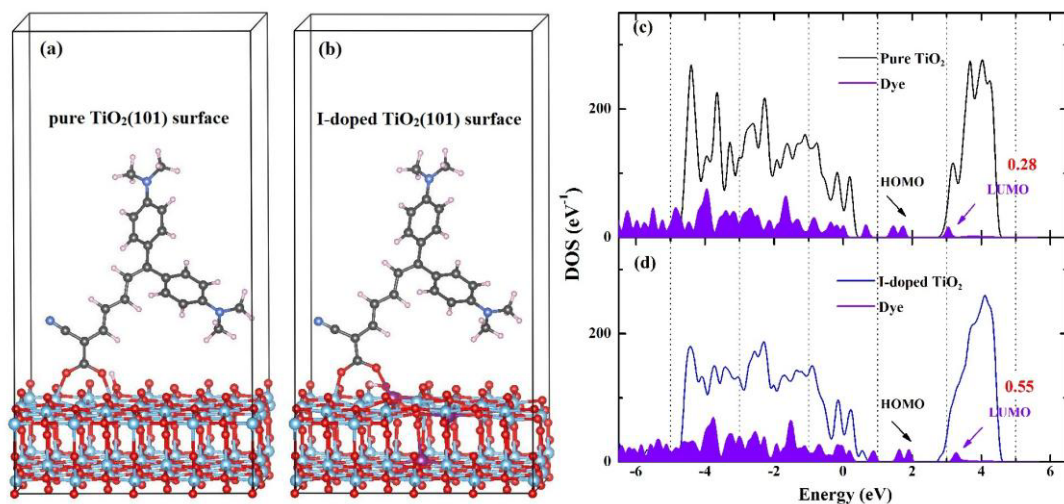


**Figure 2.** The optimized stable configuration of NKX-2554 dye adsorbed on (a) pure and (b) I-doped anatase TiO<sub>2</sub>(101) slabs. The DFT+U calculated DOSs for (c) adsorbed NKX-2554 dye/pure TiO<sub>2</sub>(101) slab and (d) adsorbed NKX-2554 dye/I-doped TiO<sub>2</sub>(101) slab.

The calculated Eads energies of these adsorption configurations indicate that the BB-type configuration is the most favorable mode of dissociative adsorption for NKX-2554 dye,[15] with a positive Eads of 1.29 eV. The optimized geometrical structure of the NKX-2554 dye adsorbed on pure and I-doped TiO<sub>2</sub>(101) slab are given in Fig. 2a and Fig. 2b, respectively. It is found that although the incorporation of I-dopants in TiO<sub>2</sub>(101) slab lead to a slight deformation of the surface structure, the stable adsorption configuration of the NKX-2554 dye is not changed compared with that of pure TiO<sub>2</sub>(101) surface.

The DFT+U calculated DOSs for the adsorbed NKX-2554 dye/TiO<sub>2</sub>(101) surface (or I-doped TiO<sub>2</sub>(101) surface) complexes are presented in Fig. 2c and Fig. 2d, respectively. As shown in Fig. 2c, the NKX-2554 dye induces sharp occupied molecular energy levels in the band gap of TiO<sub>2</sub>(101) slab after adsorption. The highest occupied molecular orbital (HOMO) of the dye is uncoupled with the valence band of the TiO<sub>2</sub> surface. However, the lowest unoccupied molecular orbital (LUMO) of the dye is coupled with the valence band of the TiO<sub>2</sub> surface. In adsorbed dye/TiO<sub>2</sub> complexes, the LUMO locates 0.28 eV above the CBM level of the TiO<sub>2</sub>(101) slab, which could facilitate a fast electron injection from the dye LUMO to the conduction band of TiO<sub>2</sub>. [16] Fig. 2d shows the DOSs plots of NKX-2554 dye adsorbed on I-doped TiO<sub>2</sub>(101) slab. Similarly, the LUMO of the dye is coupled with the valence band of the I-doped TiO<sub>2</sub>(101) surface. It is found that the dye LUMO is 0.55 eV above the CBM of I-doped TiO<sub>2</sub>(101) slab. Therefore, the I-doping in TiO<sub>2</sub> photoanode lead to the increasement of dye LUMO position, which can improve the electron injection rate and the performance of DSSCs.

## 4 Summary

In summary, we have used DFT+U calculations to explore the mechanism of IPCE enhancement in DSSCs based on I-doped anatase TiO<sub>2</sub> photoanodes. It is indicated that the I-doped anatase TiO<sub>2</sub>(101) surface show n-type metallic characteristic, which can improve the conductivity of anatase TiO<sub>2</sub>. The uphill shift of CMB position in I-doped anatase TiO<sub>2</sub>(101) surface can increase the open-circuit voltage of DSSCs. In addition, the band gap of TiO<sub>2</sub>(101) surface is effectively reduced through I-doping, and thus enhance the visible-light absorption of TiO<sub>2</sub> photoanode. Moreover, It is also found

that the I-doping in anatase TiO<sub>2</sub>(101) surface can facilitate the electron injection from the NKX-2554 dye to the TiO<sub>2</sub> substrate by analyzing the calculated electronic properties of adsorbed dye/TiO<sub>2</sub> complexes. Therefore, it is concluded that I doping can significantly enhance the IPCE of DSSCs due to the improved conductivity, increased open-circuit voltage, extended photo-response range of TiO<sub>2</sub> photoanode, and the effective electron injection of adsorbed dye/TiO<sub>2</sub> complexes.

## Acknowledgements

This work is supported by the Fundamental Research Funds for the Central Universities.

## References

1. B. O'regan, M. Grätzel, *Nature* **353**, 737(1991)
2. M. Grätzel, *Nature* **414**, 338(2001) 338-344.
3. T. Horiuchi, H. Miura, K. Sumioka, S. Uchida, *J. Am. Chem. Soc.* **126**, 12218(2004)
4. T. Ma, M. Akiyama, E. Abe, I. Imai, *Nano Lett.* **5**, 2543(2005)
5. M. Samadpour, P.P. Boix, S. Giménez, A. Irají Zad, N. Taghavinia, I. Mora-Seró, J. Bisquert, *J. Phys. Chem. C* **115**, 14400(2011)
6. Q. Hou, Y. Zheng, J.F. Chen, W. Zhou, J. Deng, X. Tao, *J. Mater. Chem.* **21**, 387(2011)
7. M. Niu, R. Cui, H. Wu, D.J. Cheng, D.P. Cao. *J. Phys. Chem. C* **119**, 13425(2015)
8. G. Kresse, J. Furthmüller, *Phys. Rev. B* **54**, 11169(1996)
9. P.E. Blöchl, *Phys. Rev. B* **50**, 17953(1994)
10. B. Hammer, L.B. Hansen, J.K. Nørskov, *Phys. Rev. B* **59**, 7413(1999)
11. C.J. Calzado, N.C. Hernández, J.F. Sanz, *Phys. Rev. B* **77**, 045118(2008)
12. F. De Angelis, S. Fantacci, A. Selloni, M.K. Nazeeruddin, M. Grätzel, *J. Phys. Chem. C* **114**, 6054(2010)
13. X. Hong, Z. Wang, W. Cai, F. Lu, J. Zhang, Y. Yang, N. Ma, Y. Liu, *Chem. Mater.* **17**, 1548(2005)
14. K. Hara, M. Kurashige, S. Ito, A. Shinpo, S. Suga, K. Sayama, H. Arakawa, *Chem. Commun.*, 252(2003)
15. K. Srinivas, K. Yesudas, K. Bhanuprakash, L. Giribabu, *J. Phys. Chem. C* **113**, 20117(2009)
16. T. Bessho, S. M. Zakeeruddin, C. Y. Yeh, E. W. G. Diau, M. Grätzel, *Angew. Chem.* **122**, 6796(2010)